Research Article | Vol. 26, No. 19 | 17 Sep 2018 | OPTICS EXPRESS 24343
Optics EXPRESS

Optimisation of ultrafast laser assisted etching in fused silica

CALUM A. ROSS,[1,*] DAVID G. MACLACHLAN,[1] DEBADITYA CHOUDHURY,[1,2] AND ROBERT R. THOMSON[1,2]

[1]*Scottish Universities Physics Alliance (SUPA), Institute of Photonics and Quantum Sciences (IPaQS), Heriot-Watt University, Edinburgh, UK*
[2]*EPSRC IRC Hub, MRC Centre for Inflammation Research, Queen's Medical Research Institute (QMRI), University of Edinburgh, Edinburgh, UK*
**cr120@hw.ac.uk*

Abstract: Ultrafast laser assisted etching (ULAE) in fused silica is an attractive technology for fabricating three-dimensional micro-components. ULAE is a two-step process whereby ultrafast laser inscription (ULI) is first used to modify the substrate material and chemical etching is then used to remove the laser modified material. In this paper, we present a detailed investigation into how the ULI parameters affect the etching rate of laser modified channels and planar surfaces written in fused silica. Recently, potassium hydroxide (KOH) has shown potential to outperform the more commonly used hydrofluoric acid (HF) as a highly selective etchant for ULAE. Here we perform a detailed comparison of HF and KOH etching after laser inscription with a wide range of ultrafast laser irradiation parameters. Etching with KOH is found to be significantly more selective, removing the laser modified material up to 955 times faster than pristine material, compared with up to 66 when using HF. Maximum etching rates for the two etchants were comparable at 320 μm/hour and 363 μm/hour for HF and KOH respectively. We further demonstrate that highly selective, isotropic etching of non-planar surfaces can be achieved by controlling the polarization state of the laser dynamically during laser inscription.

OCIS codes: (160.0160) Materials; (220.4000) Microstructure fabrication; (160.6030) Silica.

References and links

1. C. B. Schaffer, A. Brodeur, and E. Mazur, "Laser-induced breakdown and damage in bulk transparent materials induced by tightly focused femtosecond laser pulses," Meas. Sci. Technol. **12**(11), 1784–1794 (2001).
2. B. C. Stuart, M. D. Feit, S. Herman, A. M. Rubenchik, B. W. Shore, and M. D. Perry, "Nanosecond-to-femtosecond laser-induced breakdown in dielectrics," Phys. Rev. B Condens. Matter **53**(4), 1749–1761 (1996).
3. K. M. Davis, K. Miura, N. Sugimoto, and K. Hirao, "Writing waveguides in glass with a femtosecond laser," Opt. Lett. **21**(21), 1729–1731 (1996).
4. A. Marcinkevi Ius, S. Juodkazis, M. Watanabe, M. Miwa, S. Matsuo, H. Misawa, and J. Nishii, "Femtosecond laser-assisted three-dimensional microfabrication in silica," Opt. Lett. **26**(5), 277–279 (2001).
5. C. H. Lin, L. Jiang, Y. H. Chai, H. Xiao, S. J. Chen, and H. L. Tsai, "Fabrication of microlens arrays in photosensitive glass by femtosecond laser direct writing," Appl. Phys., A Mater. Sci. Process. **97**(4), 751–757 (2009).
6. D. Choudhury, A. Arriola, J. R. Allington-Smith, C. Cunningham, and R. R. Thomson, "Towards freeform microlens arrays for near infrared astronomical instruments," Proc. SPIE **9151**, 915146 (2014).
7. C. Ross, D. G. MacLachlan, D. Choudhury, and R. R. Thomson, "Towards optical quality micro-optic fabrication by direct laser writing and chemical etching," Proc. SPIE **10094**, 100940V (2017).
8. M. Haque, K. K. C. Lee, S. Ho, L. A. Fernandes, P. R. Herman, Y. Shimotsuma, K. Miura, K. Hirao, P. V. S. Marques, D. Kopf, G. Mayer, J. Albert, M. Rothhardt, C. Krafft, and J. Popp, "Chemical-assisted femtosecond laser writing of lab-in-fibers," Lab Chip **14**(19), 3817–3829 (2014).
9. D. Choudhury, W. T. Ramsay, R. Kiss, N. A. Willoughby, L. Paterson, A. K. Kar, J. Nishii, and G. Cerullo, "A 3D mammalian cell separator biochip," Lab Chip **12**(5), 948–953 (2012).
10. D. Schafer, E. A. Gibson, E. A. Salim, A. E. Palmer, R. Jimenez, and J. Squier, "Microfluidic cell counter with embedded optical fibers fabricated by femtosecond laser ablation and anodic bonding," Opt. Express **17**(8), 6068–6073 (2009).

#334715 https://doi.org/10.1364/OE.26.024343
Journal © 2018 Received 3 Jul 2018; revised 22 Aug 2018; accepted 22 Aug 2018; published 4 Sep 2018

Optics EXPRESS

11. K. Sugioka and Y. Cheng, "Femtosecond laser three-dimensional micro-and nanofabrication," Cit. Appl. Phys. Rev. J. Laser Appl. **1**, 41303–42006 (2014).
12. Y. Bellouard, A. Said, and P. Bado, "Integrating optics and micro-mechanics in a single substrate: a step toward monolithic integration in fused silica," Opt. Express **13**(17), 6635–6644 (2005).
13. Y. Cheng, K. Sugioka, and K. Midorikawa, "Microfabrication of 3D hollow structures embedded in glass by femtosecond laser for Lab-on-a-chip applications," Appl. Surf. Sci. **248**(1-4), 172–176 (2005).
14. M. Haque, K. K. C. Lee, S. Ho, L. A. Fernandes, P. R. Herman, Y. Shimotsuma, K. Miura, K. Hirao, P. V. S. Marques, D. Kopf, G. Mayer, J. Albert, M. Rothhardt, C. Krafft, and J. Popp, "Chemical-assisted femtosecond laser writing of lab-in-fibers," Lab Chip **14**(19), 3817–3829 (2014).
15. Y. Cheng, "Internal Laser Writing of High-Aspect-Ratio Microfluidic Structures in Silicate Glasses for Lab-on-a-Chip Applications," Micromachines (Basel) **8**(2), 59 (2017).
16. R. Osellame, H. J. W. M. Hoekstra, G. Cerullo, and M. Pollnau, "Femtosecond laser microstructuring: an enabling tool for optofluidic lab-on-chips," Laser Photonics Rev. **5**(3), 442–463 (2011).
17. K. Sugioka and Y. Cheng, "Ultrafast lasers-reliable tools for advanced materials processing," Light. Appl. **3**, 12 (2014).
18. F. Sima, K. Sugioka, R. M. Vázquez, R. Osellame, L. Kelemen, and P. Ormos, "Three-dimensional femtosecond laser processing for lab-on-a-chip applications," Nanophotonics **7**(3), 613–634 (2018).
19. D. M. Knotter, "Etching Mechanism of Vitreous Silicon Dioxide in HF-Based Solutions," J. Am. Chem. Soc. **122**(18), 4345–4351 (2000).
20. Y. Bellouard, A. Said, M. Dugan, and P. Bado, "Fabrication of high-aspect ratio, micro-fluidic channels and tunnels using femtosecond laser pulses and chemical etching," Opt. Express **12**(10), 2120–2129 (2004).
21. M. Hermans, "Selective, Laser-Induced Etching of Fused Silica at High Scan-Speeds Using KOH," J. Laser Micro Nanoeng. **9**(2), 126–131 (2014).
22. J. Gottmann, M. Hermans, N. Repiev, and J. Ortmann, "Selective Laser-Induced Etching of 3D Precision Quartz Glass Components for Microfluidic Applications—Up-Scaling of Complexity and Speed," Micromachines (Basel) **8**(4), 110 (2017).
23. N. Varkentina, T. Cardinal, F. Moroté, P. Mounaix, P. André, Y. Deshayes, and L. Canioni, "Examination of femtosecond laser matter interaction in multipulse regime for surface nanopatterning of vitreous substrates," Opt. Express **21**(24), 29090–29100 (2013).
24. C. Hnatovsky, R. S. Taylor, E. Simova, V. R. Bhardwaj, D. M. Rayner, and P. B. Corkum, "Polarization-selective etching in femtosecond laser-assisted microfluidic channel fabrication in fused silica," Opt. Lett. **30**(14), 1867–1869 (2005).
25. S. Kiyama, S. Matsuo, S. Hashimoto, and Y. Morihira, "Examination of Etching Agent and Etching Mechanism on Femotosecond Laser Microfabrication of Channels Inside Vitreous Silica Substrates," J. Phys. Chem. C **113**(27), 11560–11566 (2009).
26. Y. Shimotsuma, P. G. Kazansky, J. Qiu, and K. Hirao, "Self-organized nanogratings in glass irradiated by ultrashort light pulses," Phys. Rev. Lett. **91**(24), 247405 (2003).
27. D. Tan, K. N. Sharafudeen, Y. Yue, and J. Qiu, "Femtosecond laser induced phenomena in transparent solid materials: Fundamentals and applications," Prog. Mater. Sci. **76**, 154–228 (2016).
28. C. Hnatovsky, R. S. Taylor, P. P. Rajeev, E. Simova, V. R. Bhardwaj, D. M. Rayner, and P. B. Corkum, "Pulse duration dependence of femtosecond-laser-fabricated nanogratings in fused silica," Appl. Phys. Lett. **87**(1), 014104 (2005).
29. R. Taylor, C. Hnatovsky, and E. Simova, "Applications of femtosecond laser induced self-organized planar nanocracks inside fused silica glass," Laser Photonics Rev. **2**(1-2), 26–46 (2008).
30. Y. Bellouard, A. Said, M. Dugan, and P. Bado, "Fabrication of high-aspect ratio, micro-fluidic channels and tunnels using femtosecond laser pulses and chemical etching," Opt. Express **12**(10), 2120–2129 (2004).
31. H. Seidel, "Anisotropic Etching of Crystalline Silicon in Alkaline Solutions," J. Electrochem. Soc. **137**(11), 3612 (1990).
32. J. Canning, M. Lancry, K. Cook, A. Weickman, F. Brisset, and B. Poumellec, "Anatomy of a femtosecond laser processed silica waveguide Invited," Opt. Mater. Express **1**(5), 998–1008 (2011).
33. Y. Liao, W. Pan, Y. Cui, L. Qiao, Y. Bellouard, K. Sugioka, and Y. Cheng, "Formation of in-volume nanogratings with sub-100-nm periods in glass by femtosecond laser irradiation," Opt. Lett. **40**(15), 3623–3626 (2015).
34. M. Lancry, F. Brisset, and B. Poumellec, "In the Heart of Nanogratings Made up During Femtosecond Laser Irradiation," in *Advanced Photonics & Renewable Energy* (Optical Society of America, 2010), paper BWC3.
35. M. Lancry, B. Poumellec, J. Canning, K. Cook, J. C. Poulin, and F. Brisset, "Ultrafast nanoporous silica formation driven by femtosecond laser irradiation," Laser Photonics Rev. **7**(6), 953–962 (2013).
36. N. Groothoff, M. O. Hongler, P. Kazansky, and Y. Bellouard, "Transition and self-healing process between chaotic and self-organized patterns observed during femtosecond laser writing," Opt. Express **23**(13), 16993–17007 (2015).
37. S. Rajesh and Y. Bellouard, "Towards fast femtosecond laser micromachining of fused silica: The effect of deposited energy," Opt. Express **18**(20), 21490–21497 (2010).
38. A. Champion and Y. Bellouard, "Direct volume variation measurements in fused silica specimens exposed to femtosecond laser," Opt. Mater. Express **2**(6), 789 (2012).
39. C. M. Pépin, E. Block, R. Gaal, J. Nillon, C. Hoenninger, P. Gillet, and Y. Bellouard, "Silicon formation in bulk

Optics EXPRESS

silica through femtosecond laser engraving," arXiv:1806.10802 (2018).
40. O. J. Allegre, W. Perrie, K. Bauchert, D. Liu, S. P. Edwardson, G. Dearden, and K. G. Watkins, "Real-time control of polarisation in ultra-short-pulse laser micro-machining," Appl. Phys., A Mater. Sci. Process. **107**(2), 445–454 (2012).

1. Introduction

Ultrashort pulses of sub-bandgap laser light can be used to induce nonlinear photoionization when focused tightly within a dielectric material [1, 2]. This deposition of optical energy can induce a variety of highly localized modifications to the structure of the material, while leaving the surrounding material largely unaffected. The laser modification can manifest itself in several ways, including a local change to the material's refractive index [3] and/or an increase in the material's chemical etching rate [4]. Modifying a material in this way is commonly referred to as femtosecond direct laser writing (fs-DLW) or ultrafast laser inscription (ULI). Since the material modification is confined to the laser focal volume, ULI can be performed deep within a transparent substrate, with a resolution primarily determined by the pulse energy and the size and shape of the laser focus. Translating the material through the laser focus in three dimensions therefore allows for arbitrarily shaped channels, planes, or volumes to be inscribed.

When combined with wet etching, ULI can facilitate the removal of material from a bulk glass substrate. Ultrafast laser assisted etching (ULAE) is an enabling technology for the fabrication of glass micro-components such as micro-optics [5–8], microfluidics [9, 10], micromechanics [11, 12] and lab-on-chip devices [13–18]. The minimum size of components fabricated by ULAE depends not only on the size of the focal volume, but also on the selectivity of the etchant - that is, the etching rate ratio of laser irradiated material to unmodified pristine material. Unsurprisingly, the selectivity of the etching depends greatly on the laser writing parameters, including the laser pulse repetition rate, pulse energy and polarization. Along with the many irradiation parameters, the etching agent and environment can also greatly affect the etching selectivity. A commonly used and widely studied etchant for removing laser irradiated material in fused silica is hydrofluoric acid (HF). The use of HF can be desirable because the etching rate of modified material is relatively high and consistent, although HF will also etch pristine silica significantly [19]. The use of HF to preferentially etch ultrafast laser irradiated regions in fused silica was first demonstrated by Marcinkevicius et al. [4] in 2001. Using a concentration of 5% HF in aqueous solution, channels were formed with an aspect ratio of ~20, approximately equal to the selectivity. In 2004, Bellouard et al. reported the fabrication of high-aspect ratio microfluidic channels etched in 5% HF with a selectivity of ~100, corresponding to an etching rate of 300 μm/hour [20]. Now widely adopted in research, and increasingly so in industry, HF is inherently limited to relatively low ULAE selectivity due to the fast rate at which it will also etch pristine silica. More recently, potassium hydroxide (KOH) has shown potential as a highly selective laser assisted etching agent. KOH was first used to remove laser irradiated fused silica in 2009 by Kiyama et al. Using a 10 mol/L KOH solution heated to 80°C, an etching selectivity of ~350 was obtained. Hermans and Gottmann et al. report the current benchmark in ULAE selectivity for fused silica - achieving a selectivity of 1400, corresponding to an etching rate of 290 μm/hour, using a solution of 8 mol/L KOH at 85°C [21, 22].

In this paper, we present the results of a detailed parameter space investigation into the etching rate of ultrafast laser irradiated fused silica. In our investigation, we include a detailed comparison between etching with the more conventional etchant, HF, and the lesser studied KOH. Specifically, we compare 5% HF to 8 mol/L KOH. These concentrations are commonly used in the literature and were chosen because they offer a suitable trade-off between speed and control while etching. Similar studies have been reported previously, but typically explored laser modification produced within a single localized focal volume [23] or along a one-dimensional (1D) track [21, 24, 25]. Further to investigating 1D channels, we also investigate the etching rates of two-dimensional (2D) flat planar surfaces. A well-

Optics EXPRESS

documented phenomenon when performing ULI in fused silica is the formation of periodic nanoplanes, or nanogratings [26, 27]. Nanogratings have been observed to form after writing with pulse durations between 40 and 500 fs and pulse energies between 100 and 1000 nJ, depending on the pulse duration [28]. Nanogratings are aligned perpendicular to the laser polarization direction and allow, through a not yet fully understood mechanism, the etchant to penetrate quickly along the axis parallel to the gratings, but more slowly along the axis perpendicular to the gratings [24, 29]. The formation of nanogratings enables highly selective channels and planar surfaces to be fabricated because the required orientation of the laser polarization is constant. This advantage is typically lost, however, if the desired structure is curved. Here, we demonstrate a means to fabricate curved surfaces that etch isotropically while maintaining high selectivity, by controlling the laser polarization dynamically during the inscription process.

2. Investigation into etching selectivity

2.1 Apparatus

The ULI processing was performed using ultrafast laser pulses from a commercial femtosecond pulsed fibre laser (BlueCut, Menlo Systems) operating at 1030 nm. The pulse repetition rate was variable within the range of 250 kHz to 2 MHz and the pulse duration was approximately 360 fs. Power adjustment was achieved by passing the beam through a computer controlled half waveplate and a polarizing beam splitter to provide pulse energies between 50 and 526 nJ. The polarization state of the laser could be set arbitrarily using a second half waveplate and quarter waveplate within computer controlled motorized rotational mounts. In all cases, the beam was focused inside the substrate using a 0.4 NA aspheric lens (Thorlabs A110TM-B), resulting in a focused spot with a theoretical $1/e^2$ diameter of 2.19 μm and confocal parameter of 5.03 μm in fused silica (refractive index = 1.450 at 1030 nm). ULI was performed within 10 × 10 × 1 mm substrates of fused silica which were mounted on a 3-axis cross-roller-bearing translation stage with pneumatic counter balance (Alio Industries), providing 100 nm positioning resolution.

2.2 Parameter space

As stated previously, the ULI parameters that influence the material modification include the laser pulse energy, pulse duration, repetition rate and polarization, as well as the focusing NA and speed at which the sample is translated through the focus. The shape of the ULI fabricated structure will also affect the rate and homogeneity with which it is etched. To investigate this, arrays of one-dimensional channels and two-dimensional surfaces were inscribed into fused silica as depicted in Fig. 1. Each channel and surface was inscribed with a unique set of ULI parameters. Channels were inscribed by translating the substrate laterally through the laser focus in a single pass, with the scan starting with the laser focus positioned outside the substrate. Planes of ultrafast laser modified material, measuring 230 μm across (along y) and 1000 μm deep (along z), were also inscribed by raster scanning the substrate laterally through the laser focus, starting with the laser focused beneath the bottom face of the wafer. The full set of parameters investigated is presented in Table 1.

Optics EXPRESS

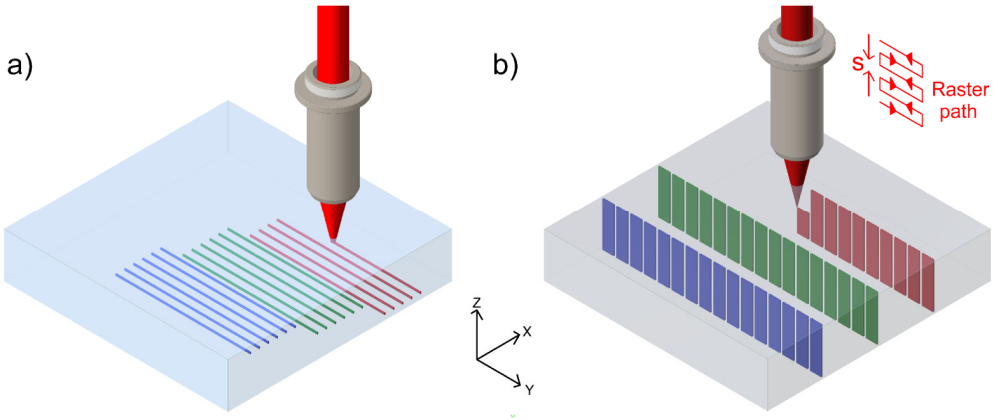

Fig. 1. Arrays of a) single scan channels and b) raster scanned planes with different scan separations (s), were inscribed in fused silica, each with unique irradiation parameters. Subsequently, substrates were etched in HF and KOH and the rate of modified material removal measured. In a), the channel colour corresponds to writing depth and in b) the surface colour denotes laser polarization during inscription.

Table 1. Summary of the ULAE parameter space investigated.

Parameter	Range	Comments
Laser source	1030 nm, 360 fs pulse duration	Constant
Pulse energy	50 – 526 nJ in increments of 18 nJ	Repetition rate dependent
Pulse repetition rate	250 kHz, 500 kHz, 1 MHz, 2 MHz	-
Laser polarization	parallel† $E_{/\!/}$, perpendicular† $E_{\perp}$, circular $E_{\circlearrowleft}$	$E_{/\!/}$ **y**, $E_{\perp}$ **x** as defined in Fig. 1
Scan separation	0.5 - 10 µm	Applies only to surfaces
Inscription depth	250, 500, 750 µm	Applies only to channels
Translation speed	0.5 mm/s	Constant
Etching agents	5% HF (40°C), 8 mol/L KOH (85°C)	-

†Linear polarization orientation stated with respect to the translation direction of the stages during inscription.

Identical laser written structures were etched in both HF and KOH for comparison. HF was diluted from a 40% stock solution down to 5 v/v %. (approx. 2.87 mol/L) concentration with deionized water. HF etching was performed in an ultrasonic cleaning bath to ensure the solution remained homogeneously concentrated for the duration of the etch. A by-product of ultrasonic mixing is heat generation. Therefore, HF etching was performed at 40 ± 2 °C - the measured equilibrium temperature of the HF in the ultrasonic bath during operation. The KOH solution was prepared by mixing stock KOH pellets with deionized water to a molar concentration of 8 mol/L (approx. 25 v/v %). The KOH solution was heated to a temperature of 85 ± 2°C on a hot plate and magnetically stirred for the duration of the etch.

The etching rate of inscribed material was obtained by measuring the penetration depth of the etchant along the channels (in the y-axis) and through the surfaces (in the z-axis, the optical axis of the laser) after 90 minutes of etching. The clear tapering of the channels in Fig. 2(a), is itself an indication of the selectivity, as it is caused by the outward etching of pristine material as the etchant propagates down the channel. In the case of surfaces, the etchant penetrated the laser modified material via both faces of the substrate, denoted here as *near* and *far,* corresponding to their proximity to the inscription lens during laser writing. A typical micrograph of inscribed channels and surfaces taken after etching is presented in Fig. 2(b).

Optics EXPRESS

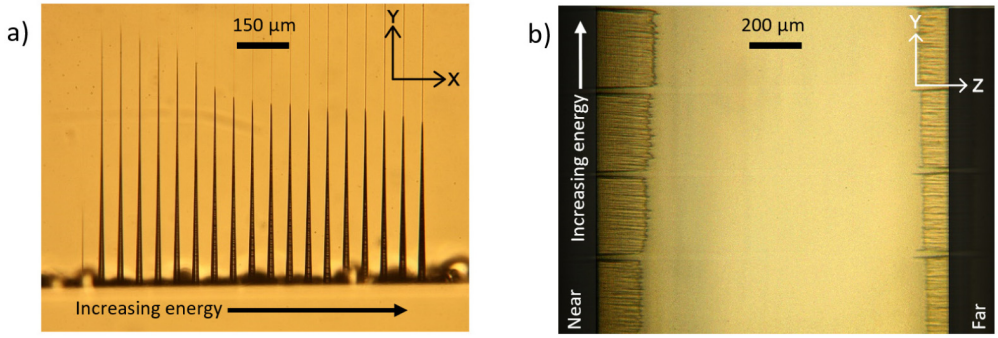

Fig. 2. (a) Micrograph of a group of single scan channels inscribed with increasing pulse energy from 50 to 526nJ and etched in a 5% HF solution for 90 minutes. Here the laser was linearly polarized along the x-axis. b) Etchant penetration into 2D surfaces inscribed with the laser polarized along the y-axis (parallel to the translation direction) and etched in 5% HF for 90 minutes. The etching agent penetrates both faces of the glass, denoted as near (left) and far (right) which corresponds to their proximity to the inscription lens during laser writing.

2.3 Etching rate of pristine silica

A precise measurement of the etching rate of the pristine material is crucial to accurately assess the selectivity with which the laser modified regions are etched. Etching of amorphous glass is inherently three dimensional. However, it is typical for the etching rate of fused silica to be described as the amount of material removal per unit time along a single etching direction. In literature, values for the etching rate of pristine fused silica vary considerably. Marcinkevicius et al. report that fused silica in a 5% HF solution will etch at a rate of approximately 4.5 µm/hour at ambient temperature [4]. Bellouard et al. provide the intrinsic etching rate under similar conditions, stating an etching rate of approximately 3 µm/hour for high purity fused silica [30]. Seidel et al. measured the etching rate of fused silica in various concentrations of KOH solution and at a range of temperatures [31]. For an 8 mol/L solution at 85°C, the etching rate was stated as being 0.6 µm/hour, noting that a temperature increase of 10 °C results in an approximate doubling of the etching rate. Hermans et al. [21] arrive at a slower intrinsic etching rate – just 0.21 ± 0.015 µm/hour for an 8 mol/L solution at 85°C; as do Kiyama et al. [25]. who measure an etching rate of 0.25 µm/hour for a 10 mol/L solution at 80 °C.

Here, pristine etching rates were determined by measuring the change in thickness of a fused silica substrate after a series of 2-hour etching periods. Etching was performed under the same conditions described in Section 2.2. After some time, the concentration of the etchant can be expected to decrease due to the ongoing reaction with the silica substrate. However, in our case the mass of silica removed was insignificant compared with the mass of the etchant solute and so any change in the concentration was negligible. In addition, new etching solutions were carefully prepared at the start of each 2-hour etching period. The temperature of the 5% HF and 8 mol/L KOH solutions were maintained at 40 ± 2 °C and 85 ± 2 °C respectively. A plot of the material removal over a 12-hour period is shown in Fig. 3. The etching rates were found to be 4.86 ± 0.04 µm/hour and 0.38 ± 0.02 µm/hour for the HF and KOH solutions respectively. We note that while the value we measured for HF is broadly in agreement with those reported by Marcinkevicius [4] and Bellouard [30], the value we measured for KOH is significantly higher than that reported by Hermans [21] and Kiyama [25].

Optics EXPRESS

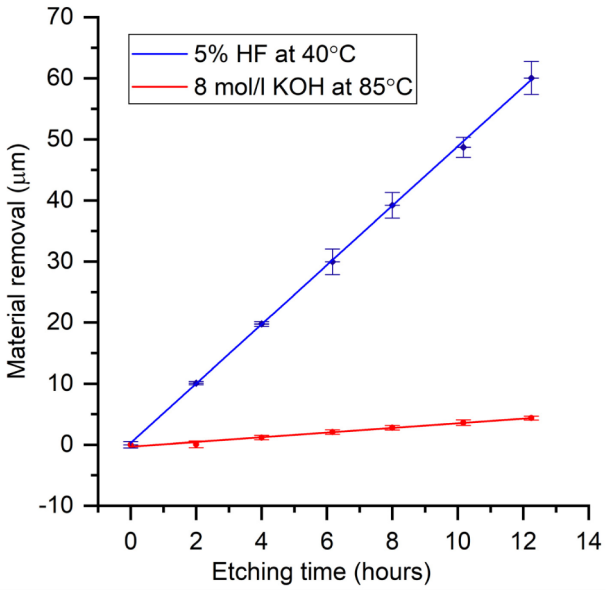

Fig. 3. Etching rate of high quality pristine fused silica submerged in HF and KOH. Etching rates in 5% HF at 40 ± 2 °C (blue line) and 8 mol/L KOH at 85 ± 2 °C (red line) were 4.86 ± 0.04 μm/hour and 0.38 ± 0.02 μm/hour respectively. Error bars represent one standard deviation determined from six repeat measurements.

2.4 Results and discussion

The etching selectivity, S, is the ratio of the etching rate of laser modified material to that of the pristine material. If after etching for some time, t, the etchant has penetrated the laser affected zone by a measured distance l, then the selectivity is given by $S = (l + \varepsilon t)/\varepsilon t$, where ε is the pristine material etching rate. The influence of the different inscription parameters on the etching selectivity is discussed, first for HF and then for KOH.

2.4.1 Hydrofluoric acid

The results of the parameter space investigation into HF are presented in Fig. 4. When using 5% HF as the etching agent, maximum etching rates of ~320 μm/hour and ~287 μm/hour were recorded for channels and surfaces respectively, corresponding to selectivities of 66 and 59. A minimum pulse energy threshold was observed at approximately 100 nJ, below which no change to the material's etching rate was observed. A steep rise in selectivity occurred for a pulse energy range between 120 and 250 nJ. This energy range corresponds to laser inscription in the regime of nanoplane formation [28], where periodic planes of oxygen deficient [32] material self-align within the focal volume - perpendicular to the incident laser polarization. Evidence suggests that nanoplanes are formed of parallel nanocracks [33] or porous silica [34, 35] which allows the etching agent to propagate more quickly through the inscribed material – explaining the sudden increase in selectivity. The selectivity was observed to level off or in some cases decrease at pulse energies beyond 250 nJ as shown in Fig. 2(a). At pulse energies above 300 nJ, the nanogratings are known to become disordered [36], potentially hindering the etchant transport through the material.

Writing at lower repetition rates favoured increased etching speed, with little difference noticed between repetition rates of 250 kHz and 500 kHz. The etching selectivity was observed to drop for repetition rates above 1 MHz, particularly at higher pulse energies. Thermal accumulation has been reported in the laser affected zone when writing with repetition rates in the MHz range [37], and this may have a role to play in disrupting the

Optics EXPRESS

formatting of the nanogratings that play a crucial role in the ULAE process. As the repetition rate increases, the total energy deposited also increases for a given pulse energy. This observation could be explained by the results from Champion et al. [38] who demonstrated that stress within the material increases with deposited pulse energy up to a maximum, at which point the etching rate is highest. After this point, stress is relieved through local fractures and the etching rate levels-off, or in some cases decreases.

The polarization state of the incident laser light was also found to significantly affect the etching rate of irradiated material. When the polarization state was linear and aligned perpendicular to the channel or surface, the etching rate was substantially increased. The average selectivity of channels inscribed and etched in HF was found to be 13.8 times greater when the polarization was aligned perpendicular to the channel than when aligned parallel to the channel. Similarly, the selectivity was increased by an average of 2.6 times for surfaces written with the polarization normal to the surface. The increase in selectivity can be attributed to the formation of nanoplanes or cracks in the same orientation as the length of the channel or the plane of the surface. When the nanogratings are formed orthogonally to the channel or surface, etching is no longer primarily facilitated by the alignment of nanocracks and so the pulse energy becomes the dominant influence on etching rate. In this case, selectivity is observed to increase with pulse energy as shown in Fig. 2(b).

Typically, the selectivity was observed to decrease as the writing depth increased. Also, a higher pulse energy threshold was observed at greater writing depths. It is well known that spherical aberration arising at the air-glass interface distorts the focal volume, and the amount of distortion increases with increasing writing depth in the sample. As the focal volume distorts, the peak intensity of the focus decreases, and we would expect the threshold pulse energy to increase, as observed.

The effect of scan separation, s (Fig. 1(b)), on the etch rate of the ULI fabricated planes, was also investigated while keeping the pulse energy and repetition rate constant. The results are presented in Fig. 4(c). As expected, the selectivity was highest when the laser polarization was aligned orthogonal to the translation direction. More interestingly, we found that the HF penetrated through the material quickly for all scan separations up to the 10 μm investigated. A large scan separation facilitates shorter fabrication times, which is desirable for scaling up fabrication.

Optics EXPRESS

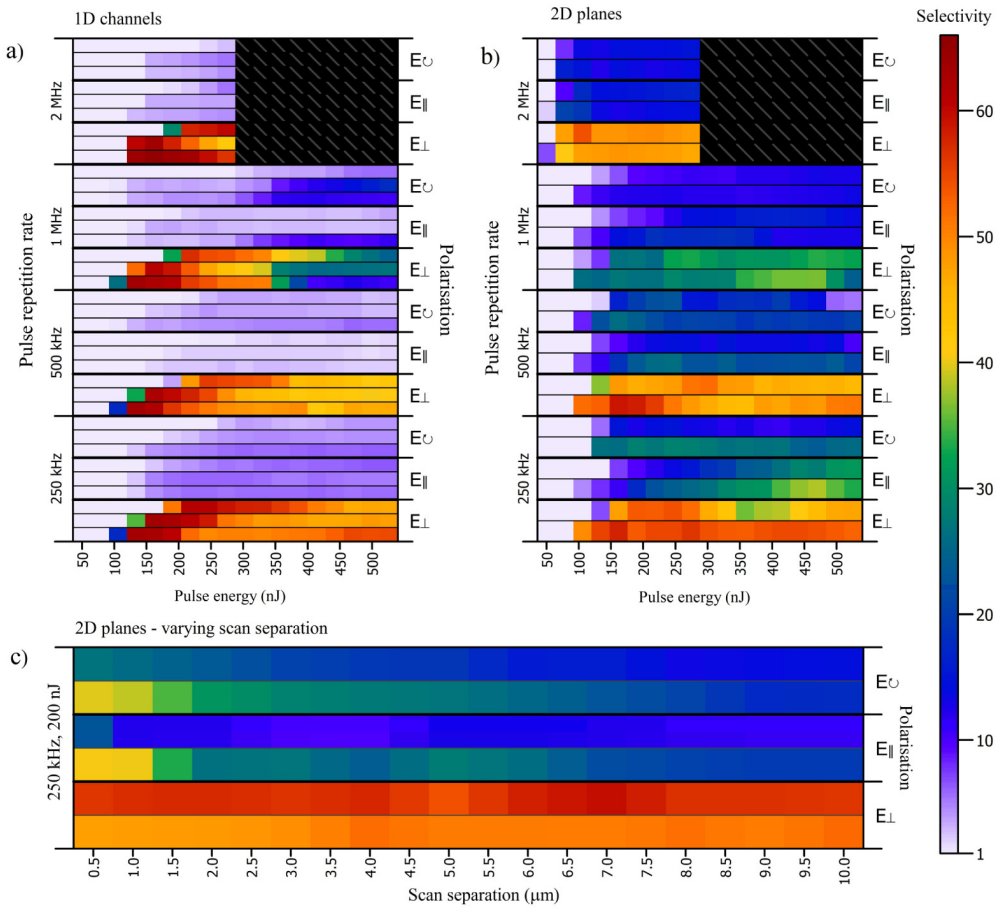

Fig. 4. Heatmaps showing the etching selectivity of laser irradiated material etched in a 5% HF solution. a) Etching selectivity of 1D channels - each triplet of rows corresponds to writing at depths of 250, 500 and 750 μm (from bottom to top on the heatmap) in bulk fused silica. b) Selectivity of 2D planar surfaces - each pair of rows represent etchant penetration into the near (bottom) and far (top) faces of the fused silica substrate, with respect to the focusing objective. In b) the surfaces were written with a fixed scan separation of 3 μm – a value well below the confocal parameter of the laser focus. Data marked with a dashed grey line were not obtained due to pulse energy limits at higher repetition rates. c) The selectivity obtained for 2D planar surfaces as a function of scan separations is presented. While the scan separation was varied, the pulse energy and repetition rate were kept constant at 200 nJ and 250kHz respectively.

2.4.2 Potassium hydroxide

The results of the parameter space investigation using KOH as the etchant are presented in Fig. 5. Etching selectivity was significantly higher when KOH was used compared to HF, with maximum etching rates of ~325 μm/hour and ~363 μm/hour measured for channels and surfaces respectively, corresponding to selectivities of 856 and 955 respectively. Similar trends in the selectivity were observed when varying the pulse energy and repetition rate and etching with KOH, as were found with HF. The effect of laser polarization on the etching rate was even more prominent when etching was carried out in KOH – with the selectivity increasing by a factor of 45.7 and 17.7 times for channels and surfaces respectively when the laser polarization was orientated perpendicular to the inscribed feature. Again, the scan separation was investigated while keeping the pulse energy and repetition rate constant at 200 nJ and 250 kHz respectively. Etching occurred faster for material that was inscribed deeper

Optics EXPRESS

within the substrate and highly selective etching was observed for laser writing with a scan separation of up to 7 µm.

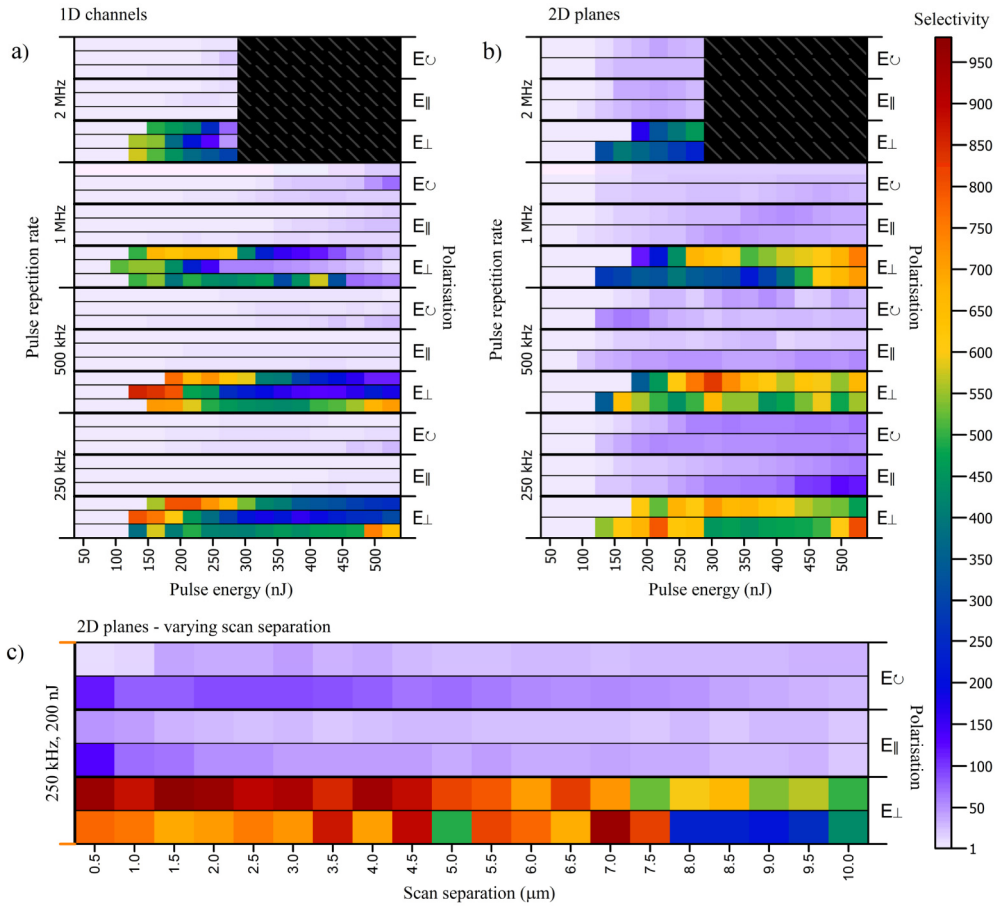

Fig. 5. Heatmaps showing the etching selectivity of laser irradiated material etched in an 8 mol/L KOH solution at 85°C. a) Selectivity of 1D channels - each triplet of rows corresponds to writing at depths of 250, 500 and 750 µm (from bottom to top on the heatmap) in bulk fused silica. b) Selectivity of 2D planar surfaces - each pair of rows represent etchant penetration into the near (bottom) and far (top) faces of the fused silica substrate, with respect to the focusing objective. In b) the surfaces were written with a fixed scan separation of 3 µm - a value well below the confocal parameter of the laser focus. Data marked with a dashed grey line were not obtained due to pulse energy limits at higher repetition rates. c) The selectivity obtained for 2D planar surfaces as a function of scan separations is presented. While the scan separation was varied, the pulse energy and repetition rate were kept constant at 200 nJ and 250kHz respectively.

The optimum parameters we found that maximized the selectivity of the etching are summarized in Table 2. Overall, the results suggest that the key factor in achieving fast etching of laser modified regions is the targeted formation of nanogratings with an orientation controlled by the laser polarization. In terms of the etching agents, KOH consistently outperformed HF in terms of selectivity by an order of magnitude. KOH has a further benefit over HF in that it is safer to work with, and hence more appealing in both research and industrial environments.

The fundamental mechanisms that drives selective etching in fused silica after ultrafast laser inscription have been a topic of much interest in recent years. Raman spectroscopy has confirmed a local decrease in the average bond angle between the silicon and oxygen atoms

Optics EXPRESS

in the tetrahedra rings that make up fused silica after laser inscription [38], and a decrease in angle has been attributed to the shortening of SiO_4 rings that leads to local material densification. The densification of silica does not explain why we observe such high selectivity when etching with KOH, which generally etches fused silica very slowly. The high selectivity can, however, potentially be explained by recent work from Pépin et al., who reported the formation of crystalline silicon within ultrafast laser inscribed fused silica [39]. Crystalline silicon is known to etch up to three orders of magnitude faster than silica [31], comparable with the selectivity of laser modified silica found here.

Table 2. Summary of ULAE parameters which optimized etching selectivity as determined by a parameter space investigation.

Parameter	Optimum	Comments
Pulse energy	200-250 nJ	Depth dependent
Pulse repetition rate	250kHz	For a translation speed of 0.5 mm/s
Laser polarization	Perpendicular $\overrightarrow{E_{\perp}}$	With respect to translation direction
Scan separation	Up to 7 μm	Applies to vertical raster scanning
Etching agent	8 mol/L potassium hydroxide (85°C)	-

3. Non-planar surfaces

The strong polarization dependence of the etching selectivity makes ULAE well suited for the fabrication of planar surfaces and linear channels where the polarization orientation is easily set orthogonal to the translation direction. It is more challenging, however, to achieve a high and isotropic etching selectivity over surfaces that are curved. This is because the orientation of the nanogratings that permit fast etching is typically set by a *static* laser polarization. If inscribing a curved path with the beam polarization set static, the nanoplanes will form unidirectionally and the etching is hindered as the nanoplane alignment becomes offset from the inscribed surface normal. Here, we demonstrate that this limitation of etching curved surfaces using a static polarization can be overcome by using a *dynamic* laser polarization state where the polarization is varied during inscription.

3.1 Methodology

Three polarization control methods were investigated for writing curved surfaces. In the first, method (i), the laser polarization was linear and constant. For the second, method (ii), alternate inscription layers were written with orthogonal linear polarization states. In the third, method (iii), the linear polarization state was rotated in real-time to maintain a perpendicular alignment to the surface, as shown in Fig. 6(b-iii). This method has previously been shown to improve the quality of laser drilling in metals and was named *polarization trepanning* by Allegre et al. [40]. The polarization state was varied by rotating a half waveplate mounted in a motorized rotation stage. For method (iii), the stage was programmed to maintain a perpendicular polarization alignment to the inscription direction to within ± 0.5°. The surfaces were inscribed through a 1 mm substrate, following the path of a quarter circle with a radius of $1/\sqrt{2}$ mm, as shown in Fig. 6(a). The scan separation was set to 3 μm and writing was performed at a speed of 0.5 mm/s. Identical sets of surfaces were etched for 90 minutes in both 5% HF and 8 mol/L KOH.

Optics EXPRESS

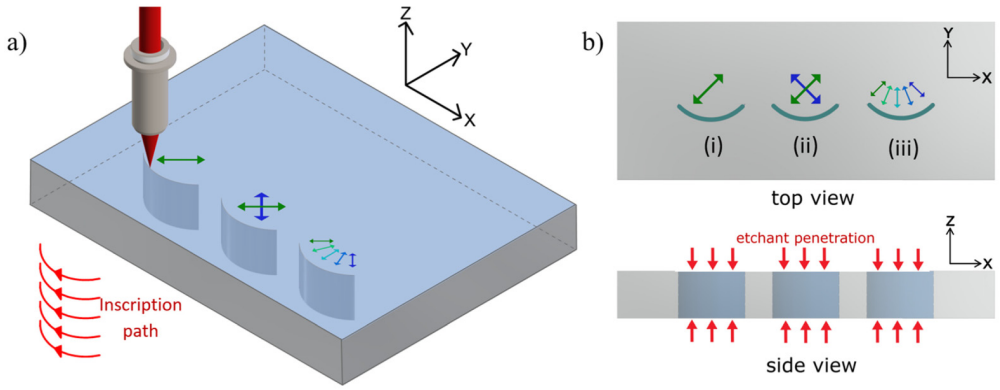

Fig. 6. An isometric view (a) and side views (b) of a schematic representing curved surfaces inscribed in a fused silica chip. Three surfaces were written using different polarization control techniques – i) static, ii) alternating orthogonal and iii) surface-matched. After inscription, the substrates were etched in HF and KOH and the etchant penetration into the top and bottom surfaces was measured.

3.2 Results and discussion

Figure 7 presents micrographs of the substrates taken in the x-z plane showing the etchant penetration into the curved surfaces after etching for 90 minutes in both HF and KOH. Figure 7(a-i) shows HF penetration into a surface written with a fixed polarization. The polarization was set orthogonal to the leftmost edge of the quarter circle, and effectively rotated with respect to the surface during translation of the stages. Consequently, etching is high initially but falls off as the polarization offset increases. The maximum etching selectivity was measured to be 64.1 ± 3.2, falling to a minimum of 12.1 ± 3.0. In Fig. 7(a-ii), the surfaces have been written with orthogonal polarization states for each alternate layer and etched in HF. Etching across the surface showed improved isotropy with an average etching selectivity of 25.0 ± 2.9. Figure 7(a-iii) presents a micrograph of the final surface etched in HF, inscribed this time with surface-matched polarization. Again, etching over the entire surface showed high isotropy, with a further improved average selectivity of 58.0 ± 3.1.

Optics EXPRESS

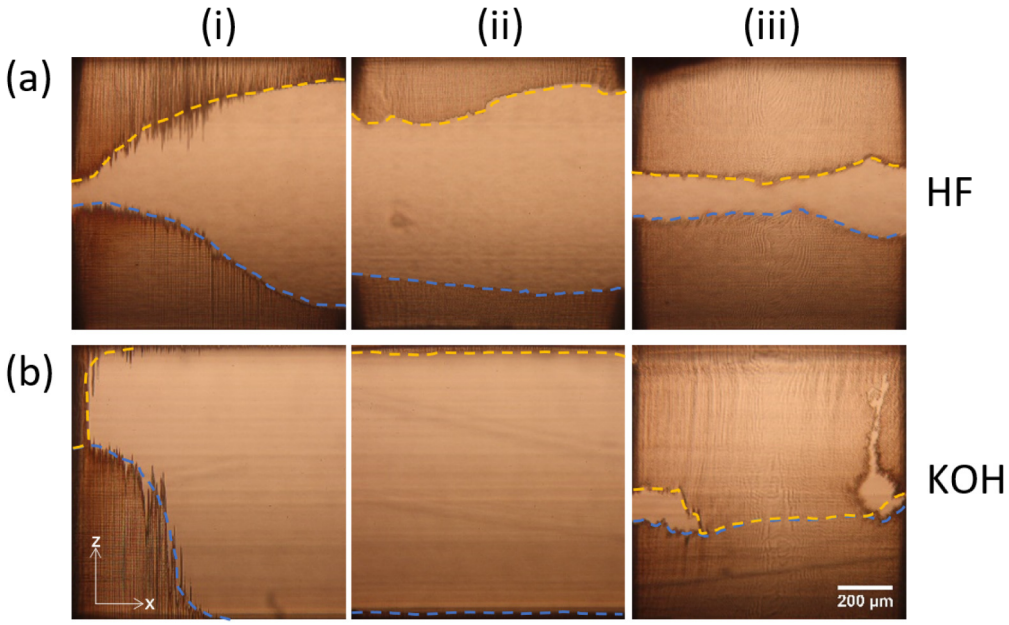

Fig. 7. Micrographs taken in the x-z plane, show the polarization dependence of etchant penetration into the near face (highlighted by a blue dotted line) and far face (highlighted by a yellow dotted line) of the substrate for each of the three polarization control cases when etching with HF and KOH.

Figure 7(b-i) shows the penetration of KOH into a quarter circle surface inscribed with fixed polarization. Again, the etching rate fell as the polarization offset increased. However, with KOH, the drop off was more abrupt, with a maximum selectivity of 889.4 ± 41.0 but no observable preferential etching occurring after polarization offset became greater than ~42°. Etchant penetration into the far side of the glass was also noticeably poorer than in the near side. It may be that the nanogratings are less well defined when written deeper in the glass due to beam aberrations, and so etching is inhibited more quickly as the polarization offset occurs. Figure 7(b-ii) shows KOH penetration into surfaces written with alternating orthogonal polarization states. Very little observable etching occurred after 90 minutes, suggesting pathways for the etchant to penetrate along were not formed. However, when the polarization was dynamically maintained as shown in Fig. 7(b-iii), etching performance was significantly improved, penetrating through the 1 mm fused silica substrate with an average selectivity of 816.5 ± 40.1.

As a proof of principle, our results show that maintaining the polarization alignment orthogonal to the surface does indeed enable highly selective and isotropic etching. The requirement to have perfectly orthogonal polarization was observed more strongly when etching in KOH than in HF. A likely explanation for this is that HF etches pristine material much more quickly than KOH, and so HF can penetrate over misaligned nanoplanes faster than KOH can. It should be highlighted that several practical challenges and limitations exist in using physical optics to synchronize laser writing with beam polarization during ULI. Firstly, there is a limit to the rate of change of direction, i.e. the curvature of a surface, set by the maximum speed of the waveplate rotation mount. An extreme example of this is when an instantaneous change in translation direction, and hence polarization angle, is required, which is not possible using physical optics. Secondly, physical rotational mounts tend to drift in reported position over time, and so multiple homing sequences must be performed during inscription. Electro-optic modulation has the potential to resolve each of these issues and presents an interesting area of research for future work.

Optics EXPRESS

4. Conclusion

In summary, optimum ULAE irradiation parameters have been found that give rise to highly selective etching of laser irradiated fused silica. The optimal parameters suggest that nanograting formation is the key driver in achieving a high etching rate. Both hydrofluoric acid and potassium hydroxide were investigated as etching agents. When using a 5% HF solution, a common fused silica etchant, a maximum selectivity of 66 was obtained corresponding to an etching rate of 320 μm/hour. We found that 8 mol/L KOH heated to 85°C performed significantly better than HF, providing a maximum etching selectivity of 955, corresponding to a comparable etching rate of 363 μm/hour.

The fabrication of curved micro-components by ULAE is typically challenging since nanoplanes fail to form a path for the etchant to penetrate along. Here we have demonstrated that varying the laser polarization orientation dynamically to ensure that the polarization remains orthogonal to the translation direction enables highly selective and isotropic etching of non-planar surfaces. These results shed light on the requirements for highly selective laser-assisted etching of fused silica and reinforce ULAE as a capable manufacturing tool for complex glass micro-components. Implementing optimal beam parameters dynamically remains an interesting control challenge in the field of laser machining.

Data

Data will be made available on the Heriot-Watt PURE system.

Funding

UK Science and Technologies Facilities Council (STFC) (ST/M007839/1); UK Engineering and Physical Sciences Research Council (EPSRC) (EP/K03197X/1); Heriot-Watt University-Renishaw Strategic Alliance.

Acknowledgements

The authors would like to thank UK Science and Technologies Facilities Council (STFC) (ST/M007839/1); UK Engineering and Physical Sciences Research Council (EPSRC) (EP/K03197X/1); and Heriot-Watt University-Renishaw Strategic Alliance.